Groundwater model parameter identification using a combination of cone-penetration tests and borehole data.

Bart Rogiers[1] , Marco Schiltz[2], Koen Beerten[3], Matej Gedeon[4], Dirk Mallants[5], Okke Batelaan[6], Alain Dassargues[7], Marijke Huysmans[8]

Abstract

In the framework of the disposal of short-lived low- and intermediate-level radioactive waste in a near-surface disposal facility in Dessel, Belgium, additional extensive site characterisation has been performed in 2008. The gathered data now include 388 hydraulic conductivity measurements on samples from 8 cored boreholes. Detailed characterisation of these cored boreholes, together with geophysical logging, enabled to identify various hydrostratigraphical units at 8 discrete locations in the research area. Various analyses were performed on the cores, yielding information on grain size, mineralogy, density and total porosity. Geophysical logging parameters were derived from gamma-ray and resistivity measurements. Subsequently, an extensive geotechnical logging campaign was performed in order to establish a 3D-model of the hydrostratigraphical units, based on a dense network of investigation points. About 180 cone penetration tests (CPTs) were executed and lithology was deduced in detail based on existing soil classification charts. As such, a description of the regional subsurface up to depths of nearly 50 m was established, and this information was integrated with the borehole data. Most importantly, the lateral extent, depth and thickness of a hydrogeologically important aquitard was identified.

Based on the 2008 site characterisation results and their interpretation, an update of a groundwater flow model used in safety assessments was made. The CPT-based stratigraphic model and the hydraulic conductivity data determined at different scales were combined into a new 3D hydrostratigraphical model. The small-scale measurements (on 100 cm^3 core samples) are compared with hydraulic conductivity values obtained from pumping tests and the large-scale parameters derived by inverse modelling. The performance of the original and the updated flow model are compared. The presented approach was succesfull in substantially decreasing the conceptual model and parameter uncertainty and resulted in an improved calibration of the groundwater flow model.

[1] PhD student, Performance Assessment Studies, Belgian Nuclear Research Centre, and Dept. of Earth and Environmental Sciences, K.U.Leuven, brogiers@sckcen.be

[2] Geologist, Samsuffit Geoservices, marco@samsuffit.be

[3] Geologist, Performance Assessment Studies, Belgian Nuclear Research Centre, kbeerten@sckcen.be

[4] Hydrogeologist, Performance Assessment Studies, Belgian Nuclear Research Centre, mgedeon@sckcen.be

[5] Head of the unit, Performance Assessment Studies, Belgian Nuclear Research Centre, dmallant@sckcen.be

[6] Professor, Dept. of Earth and Environmental Sciences, K.U.Leuven, and Dept. of Hydrology and Hydraulic Engineering, Vrije Universiteit Brussel, batelaan@vub.ac.be

[7] Professor, Dept. of Earth and Environmental Sciences, K.U.Leuven, and Dept. of Architecture, Geology, Environment and Civil Engineering (ArGEnCo), Université de Liège, alain.dassargues@ulg.ac.be

[8] Postdoctoral researcher, Dept. of Earth and Environmental Sciences, K.U.Leuven, marijke.huysmans@ees.kuleuven.be

1 Introduction

In the framework of developing a surface repository for low and intermediate level short-lived radioactive waste in Belgium, many hydrogeological studies have been performed since 1985 in the Mol-Dessel area (Figure 1). Several studies emphasized the need to represent in detail the hydrostratigraphy of the two aquifers above the regional Boom aquiclude in the models for flow and transport simulations. A particular concern was to reproduce accurately the role of the semi-pervious clay-rich layer called the Kasterlee Clay, which forms an aquitard between both aquifers. The thickness, composition, and hydraulic properties of this layer are quite heterogeneous and need to be well defined given its important role in the flow and transport processes at the disposal site and its surroundings. Previous modelling work (Gedeon & Mallants, 2004) recommended further site investigation mainly to reduce uncertainties related to the Kasterlee Clay aquitard.

In 2007, further hydrogeological modelling was performed in order to provide specific recommendations for the 2008 site characterisation campaign (Gedeon & Mallants, 2007). Sensitivity analyses were performed to 1) delineate areas where further investigations were needed and 2) propose a spatial sampling of hydrogeological parameters to reduce model uncertainties (Gedeon & Mallants, 2010).

The gathered data now enclose 388 hydraulic conductivity measurements on samples from 8 cored boreholes (Figure 1), representing 400 m of continuous core material. Various analyses were performed on the cores, yielding information on grain size, mineralogy, density and total porosity. Geophysical logging parameters were derived from gamma-ray and resistivity measurements. Several pumping tests were performed and interpreted. Subsequently, an extensive geotechnical logging campaign was performed with about 180 cone penetration tests (CPTs; Figure 1). For details, the reader is referred to Wemaere et al. (2010).

This paper describes the results of interpretations of the newly collected data and discusses the consequences their implementation has for the groundwater flow modelling.

2 Data and stratigraphical interpretation

2.1 Cored boreholes

The location of the 8 cored boreholes (Dessel-2, Dessel-3, etc.) is given in Figure 1. The 50-m long cores were taken with a pushing corer operated from a drilling platform. It is a well suited technique for coring soft sediments with high recovery and low disturbances. The fairly undisturbed cores were retrieved in a PVC tube of about 1 to 1.10 m length and an inside diameter of 96 mm. In addition, well logging was performed, including gamma-spectrometry and resistivity measurements. Pumping tests were also performed at all borehole locations with filter sections at various depths (principally above and below the aquitard).

A number of analyses were performed on the borehole core samples. Grain-size measurements were done by means of two different techniques: a detailed analysis using a sedigraph yielding 20 sample fractions and a standard sieving method yielding 8 size fractions.

Dry bulk density, expressed as dry weight per sample volume (g/cm^3) was determined according to the European standard EN 1097 for 157 samples (100 cm^3 sample volume). The total porosity expressed in volume percent (cm^3/cm^3) was determined on the same samples with the pycnometer method according to the EN 1097-6 standard. Additional measurements of the bulk density were made on about 34 plugs of known volume (60 cm^3) after drying them during more than 24 hours at 100 °C. Prior to determining bulk density and total porosity (based on weight loss from saturated samples), the plugs were used to determine saturated hydraulic conductivity.

Saturated hydraulic conductivity was also measured on core material using 100 cm^3 (permeameter with constant head), 60 cm^3 (low to medium K permeameter) and 4000 cm^3 (permeameter for 0.5-m long undisturbed core sections containing alternating layers of sand and clay) samples. The latter two sample sizes were mainly used for clay-rich samples.
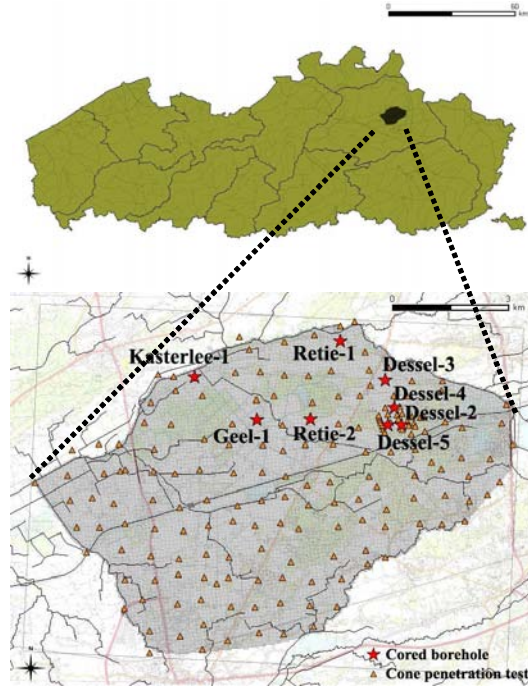
Figure 1: Location of the study area within the watersheds of Flanders and the study area with the locations of the cored boreholes (stars and borehole names indicated as Dessel-2,...) and CPTs (triangles).

Glauconite content was analysed within the grain size fraction between 50 and 500 µm using a Frantz Magnetic Barrier Laboratory Separator. In several cases, the magnetic fraction contained additional minerals to glauconite. Therefore an additional analysis was needed to estimate the real amount of glauconite by means of a stereo microscope. The glauconite content is expressed in percent of total weight of the fraction between 50 and 500 µm.

The cation exchange capacity was determined with colorimetry (spectro photometry) according to ISO/DIS 23470 (extinction at 475 nm).

2.2 Stratigraphical model

The stratigraphy is essentially based on the interpretation of borehole Dessel-2 which was the first of the 8 locations to be cored and described (Louwye et al., 2007). In addition to the compilation of data shown in Figure 2 and 3, dinoflagellate cyst identification of several layers helped identifying their respective stratigraphic position. The lithostratigraphy shown here, with both formal and informal formation names, then served as a basis for interpretation of the other 7 cored boreholes.

In total, 7 different stratigraphic units are distinguished (described here from top to bottom; except for the top unit, all other units are of Pliocene age). Quaternary wind-blown deposits of variable thickness with soil development are present all over the site. The well-known white to pale-yellow medium to coarse quartz sands (250-500 µm) attributed to the Mol Formation were identified in the Dessel cores (Dessel-2, -3, -4) right underneath the Quaternary deposits. The unit is labelled 'Upper Mol' (after 'Mol Supérieur'; see discussion and references in Louwye et al., 2007). The gamma-log (γ) shows low values while the opposite is true for the resistivity-log (ρ). In the western part of the study area (i.e. boreholes Kasterlee-1, Geel-1, Retie-1 and Retie-2), the upper Pliocene strata are characterised by a greenish medium sand, with patches of white sand (Mol-like appearance). Typically, this unit is characterised by a basal gravel layer (sometimes with clay matrix) which shows a distinct

peak in the gamma-log. At present, the data are not conclusive regarding their exact stratigraphic position because these sands can either belong to the Mol Formation, the Poederlee Formation or the Brasschaat Formation. Untill further evidence becomes available, this unit is named Mol-Poederlee-Brasschaat. In several boreholes (most notably Dessel-3 and Retie-1), clayey sediments have been encountered around the transition between 'Upper-Mol' and 'Lower-Mol' (see further). It is noted that such clay intercalations have shown to be an important hydrogeological barrier in the pumping tests. Such impeding layers were however not observed in boreholes on the disposal site (Dessel-2) or in the vicinity of the site (Dessel-3, Dessel-4).

The layers mentioned so far are characterised by the presence of an important coarse sand fraction (250-500 µm), which distinguishes them from the underlying well-sorted sands (100-250 µm) with sparse and very thin clay layers that exist untill the distinct clay-rich layers of the Kasterlee Clay. These sands can be attributed to the Mol or Kasterlee Formation. The interpretation of the Dessel-2 borehole in Louwye et al. (2007) was followed, where the upper part of this unit is called 'Mol Inférieur' ('Lower Mol') while the lower part is attributed to the sandy part of the Kasterlee Formation. However, the boundary is not always very clear and may be somewhat arbitrary in some cases. According to the Dessel-2 data, the lower boundary of the Kasterlee Formation sandy top can be identified by its higher values in the resitivity-log, starting from the very low resistivity-values of the underlying clay layers, in combination with decreasing values of the gamma log. In borehole descriptions, this unit often appears as a greyish sand with some thin clay lenses.

The next unit is the informally named Kasterlee Clay (formally part of the Kasterlee Formation) and appears as a typical green unit with alternating sand and clay layers, the latter being up to 10 cm thick. The unit can easily be identified because of its very high gamma-log values and low resistivity-log values.

The sands underlying the Kasterlee Clay are attributed to the Diest Formation. The boundary with the Kasterlee Clay is based on the appearance of an important sand fraction (250-500 µm) that coincide with a change in colour. This was recognised on a visual inspection of the cores as well as in the grain-size distribution analyses. Glauconite content in the Diest Sands is also higher (10-15%) in comparison with the Kasterlee Formation (less than 1%). The Diest Formation can be subdivided into two units. The upper clayey zone is characterised by an increased clay content relative to the loosely packed glauconite-rich sands found in the lower part. The clay content in the upper part may be up to 10%, while the total fraction of fine particles (i.e. < 62 µm) may be up to 30%. The lower boundary of this clayey top zone is however not always very clear.

The sandy part of the Diest Formation (below the clayey zone) is characterised by loose brown-green medium to coarse sands with high glauconite content. The sandy part of the Diest Formation was always in the bottom of the borehole but extends further down over several tens of meters. Typically, the gamma-log shows intermediate values (lower than the clayey zone) while resistivity values are fairly low. Note that this unit is not visible in Figures 2 and 3, because it was not observed in the Dessel-2 borehole. It could, however, clearly be identified in the other drillings.

The main site characterisation efforts were put into the units described above. However, the Dessel, Berchem and Voort sands are also represented in the groundwater flow model. For a description of these units, the reader is referred to Wemaere et al. (2010).

2.3   Cone penetration tests

The cone penetration test (CPT) consists of pushing a standarised cone into the ground with a series of extension rods at a constant rate of 2 cm/sec. During penetration of the cone continuous measurements are made of resistance to penetration of the cone tip (cone resistance q_c) and of the friction along a surface sleeve just above the cone tip (sleeve friction f_s).

These tests are very convenient to determine the nature and sequence of the subsurface strata and their physical and mechanical properties. The advantage of these tests is the fast and continuous profiling, the repeatable and non-operator-dependent data and the strong theoretical basis for interpretations.
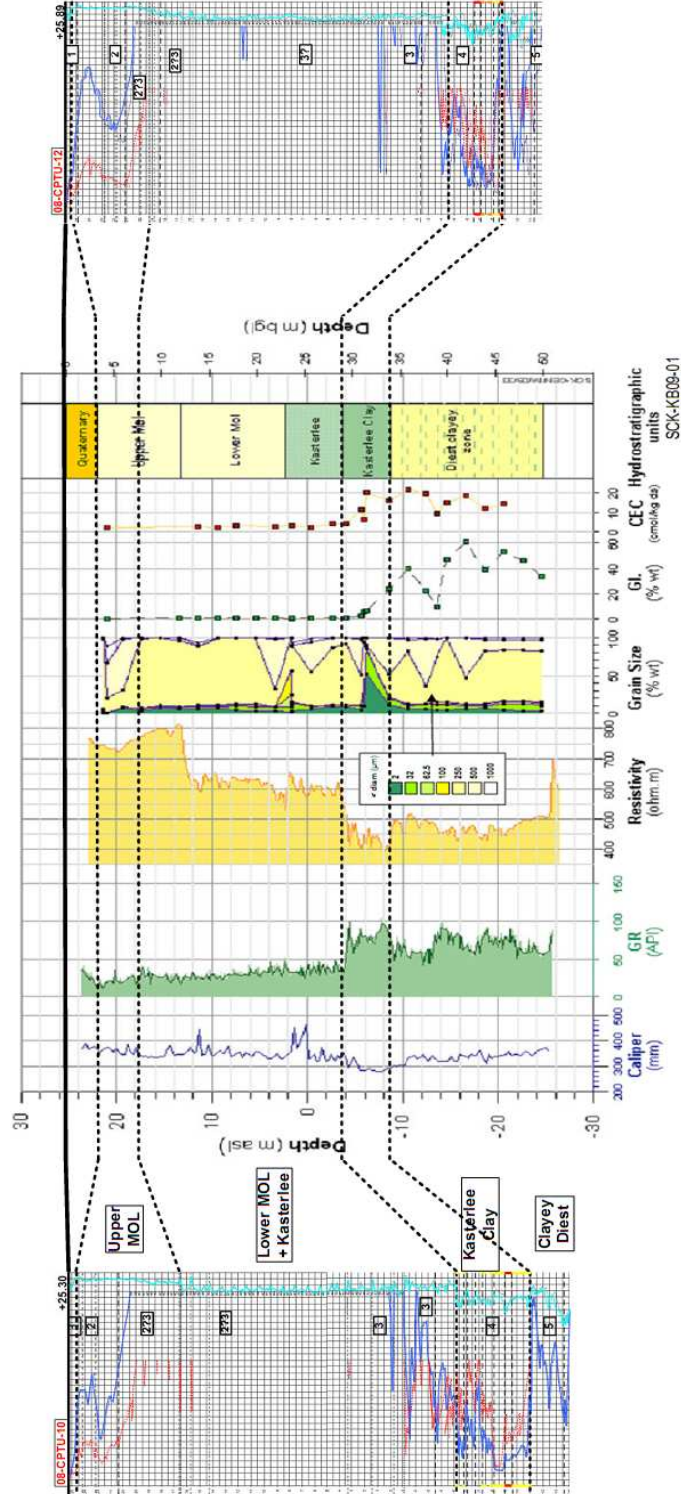
Figure 2: Results of core analyses and geophysical logging of borehole Dessel-2, and the correlation with results of two neighbouring CPT's (Wemaere et al., 2010).
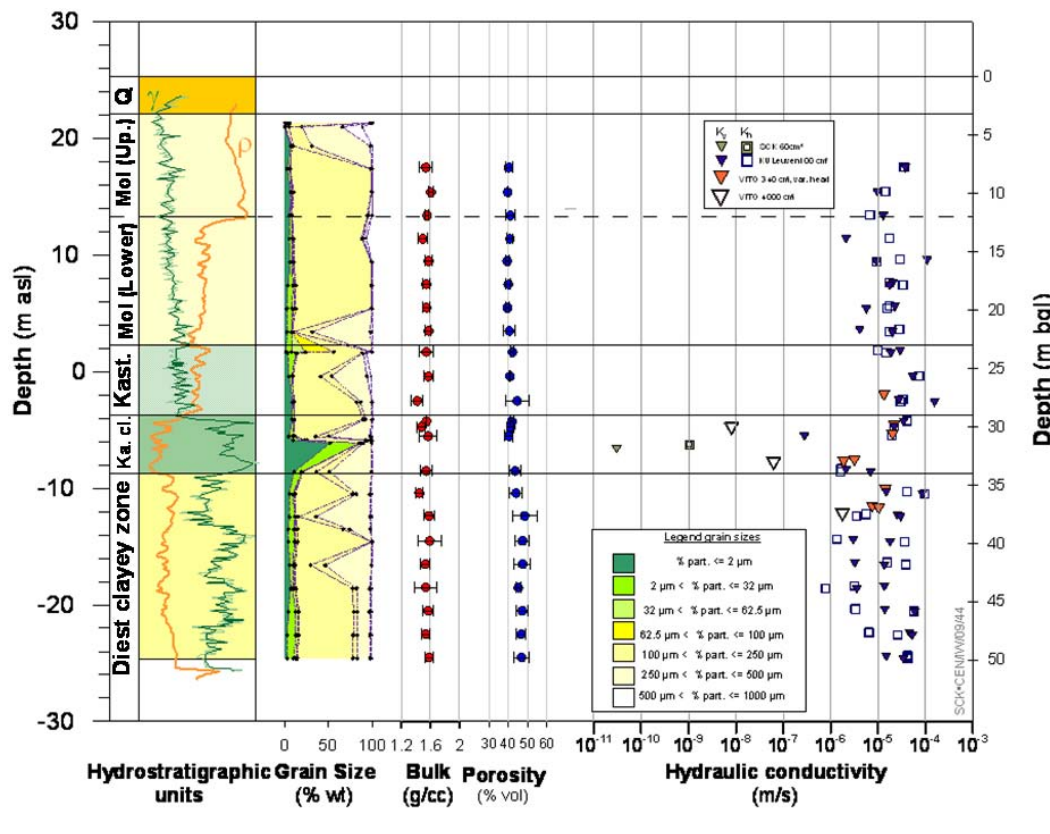
Figure 3: Hydrostratigraphy, grain size, bulk density, porosity and hydraulic conductivity of borehole Dessel-2 (Wemaere et al., 2010).
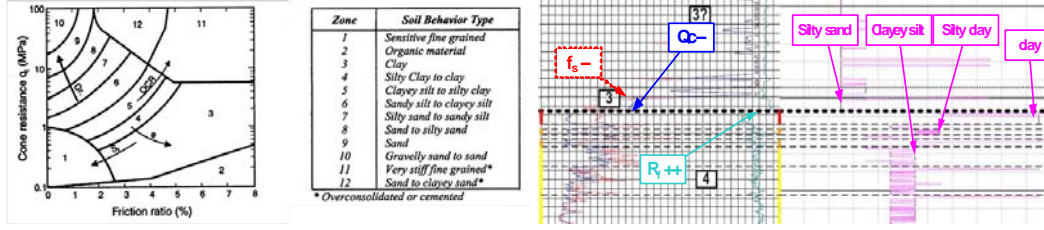
Figure 4: Left: Soil behaviour type classification for standard electric CPT (Robertson & Campanella 1986). Right: CPT- and soil chart response at the boundary between Lower Mol-Kasterlee Sand and Kasterlee Clay.

Stratigraphical unit	Lower boundary			Global unit			
	q_c	f_s	R_f	Soil (behaviour) type	q_c	f_s	R_f
Upper Mol Sands	++	++	+	Gravelly sand, sand	8-30 MPa	low	1%
Lower Mol-Kasterlee Sands	--	--	++	Silty sand, overconsolidated clayey sand	10-65 MPa	High	2%
Kasterlee Clay	++	++	++	Clayey silt, silty clay, clay	2->20 MPa	Variable	1-5%
Clayey Diest	+		-	Stiff, overconsolidated fine soils	10-30 MPa	High	5%
Diest Sands				Overconsolidated clayey sands and sands	<40 MPa	High	2-3%

++: sharp rise, +: remarked rise, -: remarked drop, --; sharp drop

Table 1: Geotechnical characteristics of the different units based on CPT parameters.

The CPTs were executed in a regular grid (approximately every 750 m) in the nearly 60 km² large investigation area (Figure 1). Because of the large number of CPTs (≈180) in a reasonably restricted area and the importance to have a more accurate characterisation of the stratigraphy, especially for the Kasterlee Clay aquitard representing the transition between Diest Sands and Kasterlee Sands, the interpretation of the CPTs included stratigraphy and lithology. This characterisation could be realised partly by using typical CPT parameters like changes in pattern and value of cone resistance, sleeve friction and/or friction ratio. The new approach consists of the determination of lithology on the basis of the soil classification method of Robertson & Campanella (1986) for CPTs (Figure 4). This soil classification chart uses the basic parameters of cone resistance (q_c) and friction ratio ($R_f = q_c/f_s$).

Close to every cored and logged drilling at least one CPT was carried out, in order to "calibrate" CPT data with data from logging or lab results on cores.

Based on a systematic analysis of the calibrated CPTs, 5 out of 7 stratigraphical units could be characterised with more accuracy (Figure 4). Indeed, Table 1 summarises the characteristics of the different units and their boundaries, based on the CPTs, their lithological interpretation (soil behaviour type is based on the work of Robertson & Campanella 1986), and correlation with the cored drillings and neighbouring CPTs, the cross sections and the isohyps maps of the base of the units.

Especially the lithological interpretation of the CPT data is useful as it gives an estimate of the sand, silt and clay fractions in a continuous way.

3 Exploratory analysis of K-data

Laboratory measurements of hydraulic conductivity on the core samples are representative for a relatively small volume of the sediment. Therefore, given the inherent spatial variability in hydraulic conductivity of the subsurface (Koltermann & Gorelick 1996), such values are considered as point values and hence are not representative for the scale of the model grid applied in a groundwater flow model. To overcome this drawback, a high sampling density for each borehole was applied in the

7

current site characterisation campaign. This allowed analysis of the hydraulic conductivity variability in the vertical direction and between the sampled boreholes. An exploratory and structural data analysis was applied to the laboratory measured hydraulic conductivity values to validate the existing hydrostratigraphy, derived from the litho- and chrono-stratigraphy, and to support the derivation of representative large-scale parameters for groundwater modelling. The analysis was performed on log-transformed values, assuming a lognormal distribution of the hydraulic conductivity values.

3.1 Statistical characterisation

The statistical characterisation of the dataset consisted of descriptive statistics, and statistical testing. The latter was used to test the sample-scale anisotropy by comparing the horizontal and the vertical hydraulic conductivity measurements. The unpaired t-test was used to determine if the two population means are equal, and the variance equality was checked first by using a two-tailed F-test. Another use of these tests was to decide whether to consider the upper aquifer as a whole, assuming that it is fairly homogeneous, or to subdivide it in its sub-units according to the updated (hydro)stratigraphic model.

Several interesting results were obtained from this exploratory analysis. First of all, three hydraulic conductivity classes were identified. Figure 5 displays the histogram of the entire dataset (K_h & K_v). Three classes of $\log_{10}K$ values are clearly distinguishable. The lowest class consists of $\log_{10}K$ values between -8 and -11 $\log(m/s)$. These represent the pure clay samples which are only found in the Kasterlee Clay aquitard. The highest class represents $\log_{10}K$ values from -6.5 to -2.5 and has a mean of about -5 $\log(m/s)$. It represents the conductive sands of both the upper and lower aquifer, but also contains about one third of the Kasterlee Clay aquitard samples. The third class has a mean $\log_{10}K$ around -7 and corresponds to the less conductive clayey sand samples, which are present in each unit. The upper and lower aquifer K-values show more or less a normal distribution, while the Kasterlee Clay aquitard has a distinct tri-modal distribution. It seems thus far more heterogeneous than the other units.

Statistical testing of the K_h and K_v populations demonstrated that there is no significant anisotropy at the sample scale for the upper aquifer and the aquitard. Because K_h and K_v samples were always taken about 10 cm apart, this suggests that small-scale variability is more important than the anisotropy. The paired values are plotted in Figure 6 for the three units. Though the majority of the plotted points show a smaller K_v than K_h value, anisotropy is only significant for the lower aquifer. It is also remarkable that there are several sample pairs for which the log10 K_v value is more than 10% larger than the log10 K_h, which again supports the assumption on the small-scale variability.

The statistical testing between the upper aquifer sub-units also showed no significant differences, except when done for the Dessel-4 borehole separately (results not shown). A systematic difference between the sub-units is thus clearly not present.

3.2 Analysis of stationarity

Exploratory data analyses that rely on graphing are especially suited for spatial data (Mohanty & Kanwar 1994). Checking the stationarity of the mean and the variance of the data through suitable plots and graphs yields valuable insights into the problem and facilitates analysis and interpretation. Plots of mean versus variance based on a moving window of 5 adjacent data points were prepared in order to check the stationarity. Median versus interquartile range-squared plots are another, more robust option, due to a lesser sensitivity to outliers (Hamlett et al. (1986) and Mohanty et al. (1991)). This more robust method is however not shown, since the extreme values are an important part of the unit characteristics. Figure 7 displays the mean versus variance plots for the entire dataset. The distinct character of the aquitard is clearly visible. The windows containing data from this unit have a lower mean and a higher variance. This is due to the strong heterogeneous nature of this unit. In fact, it is an alternation of thin sand and clay sub-layers, which causes the variance to increase. The points representing the upper and the lower aquifer situated within the cloud of points representing the aquitard are coming from the border of these units with the aquitard, where the moving window
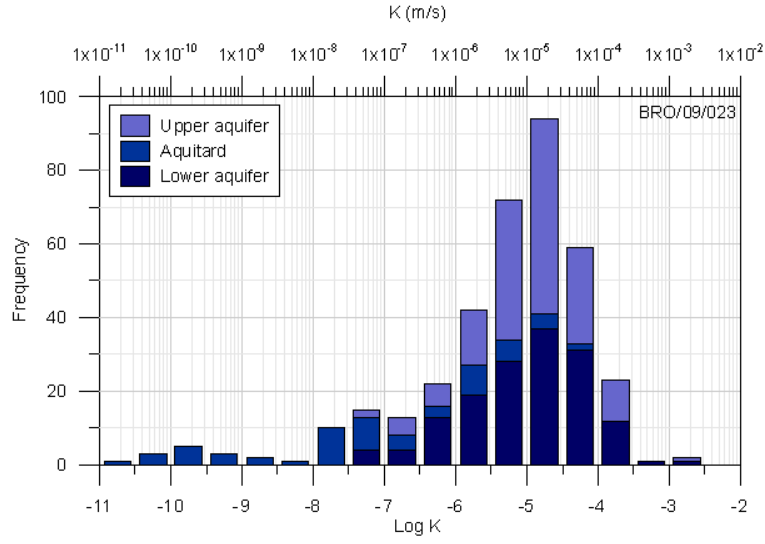
8

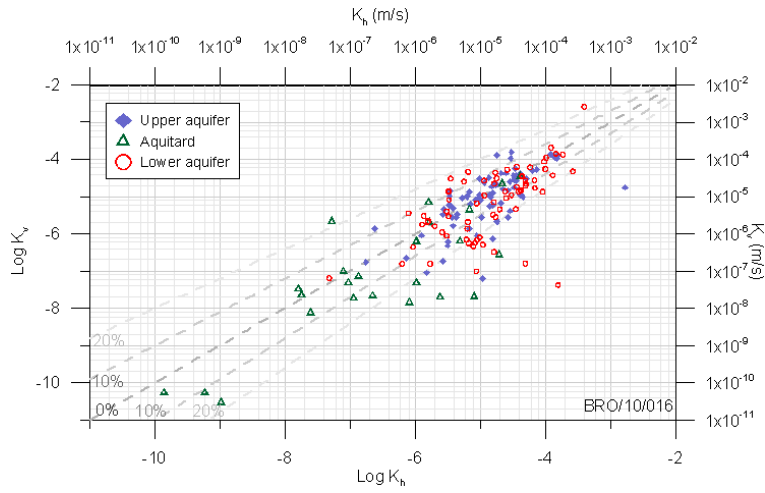Figure 5: Histogram of all K data analysed (both Kh and Kv) (Wemaere et al., 2010).

Figure 6: Log10(Kh) versus log10(Kv) plot of the paired samples (depth difference ~ 10 cm) (Wemaere et al., 2010).
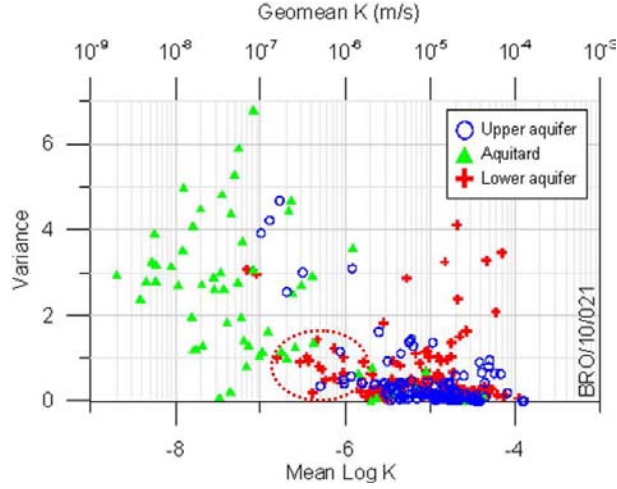
Figure 7: Mean versus variance plot for the three hydrogeologic units (joint Kh and Kv). A moving window of 5 data points was used (Wemaere et al., 2010).

includes values of both. The characteristics of the upper and lower aquifer are more or less the same. However, some low mean log K points are present within the lower aquifer (red dotted circle in Figure 7). These correspond to the clayey top of this unit, which is confirmed by the separate analyses of the Kh and Kv datasets and the borehole grain size analysis. The lower boundary of this sub-unit was hence traced separately within the stratigraphical model, as discussed earlier. The high mean log K, high variance values of the lower aquifer only occur in one single borehole, and are considered to be a random phenomenon.

The upper aquifer and the aquitard can be considered stationary as the variance is independent of the mean. Except for a few outliers, they show a fairly stationary structure. On the other hand, the upper clayey part of the lower aquifer should be treated with caution. It seems not to be consistent with the remaining part of this unit and the option should be left open to treat it separately in e.g. model calibration.

4 Updating the groundwater flow model

4.1 Model geometry

The hydrostratigraphical interpretation of the cone penetration tests was used to derive the start and end depths of the main 4 stratigraphical units at 179 discrete locations within the local model area. These units are the Quaternary and Upper Mol sands, Lower Mol sands and Kasterlee Sands, Kasterlee Clay, clayey top of Diest and Diest sands. Developing continuous surfaces of the boundaries between these units for use in groundwater flow modelling requires some spatial interpolation technique. Because kriging accounts for the spatial variability of the data, and provides a 'best estimate' in terms of the error variance, this method is preferred over more classical interpolation techniques such as inverse distance weighting. The methodology used for each of the 4 surfaces is the same and is illustrated for the top of the Kasterlee Clay aquitard.

Because of the presence of a north-northeast trend in the surface of the top of the Kasterlee Clay aquitard, a polynomial trend of 2nd order was fitted to the data (Figure 8). This trend was subtracted from the original data, and further geostatistical analysis was done on the residuals. Next, an omnidirectional semi-variogram was calculated because most of the anisotropy disappeared with removal of the trend, and a spherical model was fitted (Figure 8). The semivariance values at the higher lag distances with less than 30 data pairs were not considered when fitting the model. A leave-

Stratigraphic surface for top of:	Cross-validation error		
	AE (m)	MSE (m²)	MSNE
Lower Mol sands	-0.03	2.31	1.09
Kasterlee Clay aquitard	0.05	1.5	0.95
Diest clayey top	0	2.82	1.68
Diest sands	-0.43	8.02	1.03

Table 2: Cross-validation error measures for each of the interpolated surfaces (AE: average error, MSE: mean squared error, MSNE: mean squared normalized error).
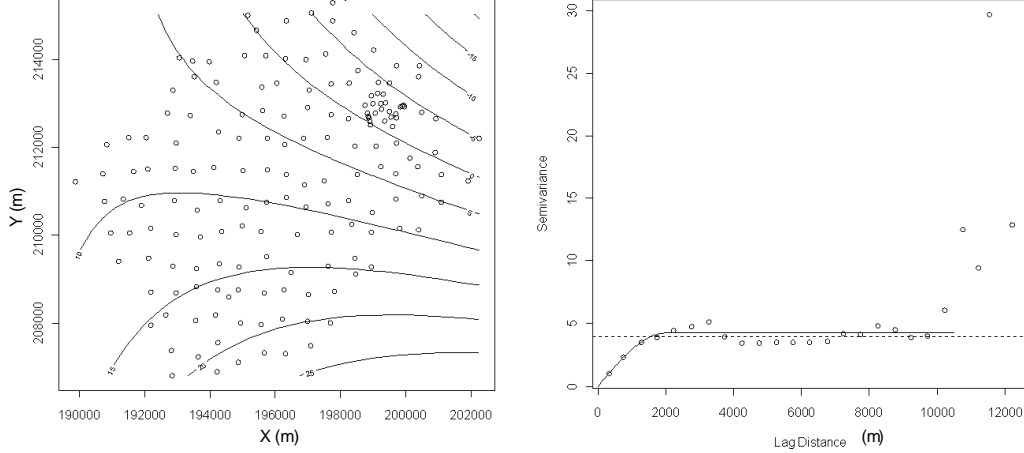

Figure 8: Left: CPT locations and contours of the polynomial trend (-1.7e+04 + 1.3e-01 * x -9.5e-08 * x² + 4.3e-02 * y -4.4e-07 * xy + 9.5e-08 * y² for the surface of the Kasterlee Clay aquitard). Right: Omnidirectional variogram of the residuals (spherical model, nugget: 0, sill: 4.26, range: 1990).

one-out crossvalidation was performed to determine the performance of the used method. The average errors are shown in Table 2. The values are fairly good given the range of 30 meter (for the top of the aquitard) and a distance of 500 to 1000 m between most CPTs and their nearest neighbours. Finally simple kriging was used to interpolate the residuals, and the result was added to the polynomial trend. Figure 9 shows the final result, and compares it with the inverse distance weighting (IDW) technique. It seems that incorporating the spatial variability yields smoother results and avoids the creation of artefacts as bull's eyes, which are abundantly present in the IDW interpolation. In the end, the top of the Diest sands surface was rejected because too little CPTs reached this surface, and extrapolation was adapted manually.

4.2 Parameterization of hydrostratigraphic units

Since a detailed 3D geometry of stratigraphic layers has been determined, it was chosen to define the hydrogeologic model independently from the numerical mesh using the MODFLOW HUF (hydrogeologic unit flow) package (Anderman & Hill, 2000). This approach allowed to define complex and realistic hydrogeologic unit geometries while maintaining a sound numerical framework (Figure 10). For example, a thin clay layer between Mol Upper and Mol Lower, with limited spatial extend was included in the model (not visible on Figure 10). The hydraulic conductivities defined in the hydrogeologic models are then converted into conductances in the numerical cells.

The use of the HUF package allowed to define the same amount of hydrostratigraphic units as identified by the site characterisation, combined with the deeper units Dessel sands and Berchem
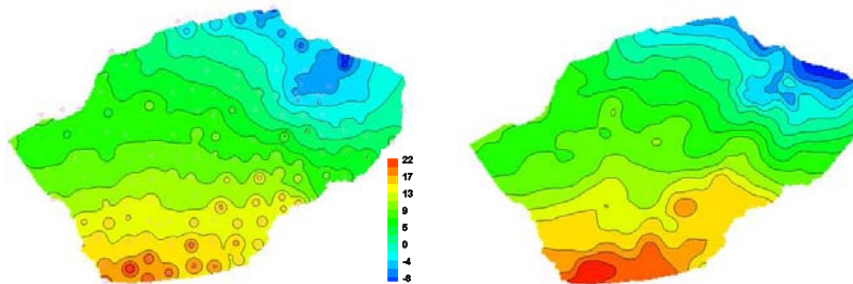
Figure 9: Topography of the Kasterlee Clay aquitard (in m above sea level) Left: Inverse distance weighted interpolation. Right: Polynomial trend and simple kriging of the residuals.
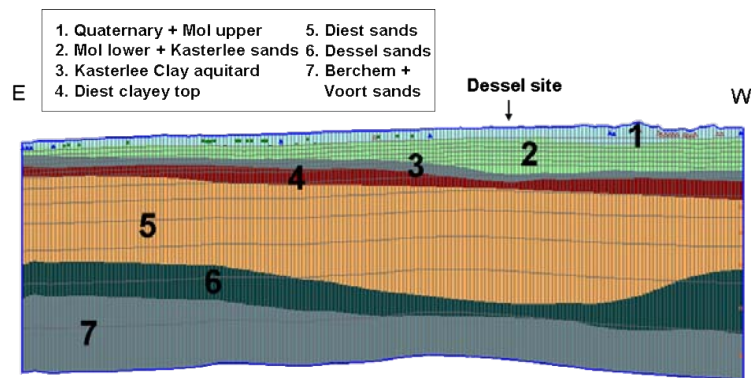

Figure 10: Typical East-West cross-section with hydrogeologic units. Combination of the hydrogeologic model and the numerical mesh using the HUF package.

Combined parameter	Hydrogeologic unit parameter	Ratio to combined parameter
	Quaternary + Mol Upper sands	0.6
	Mol clayey layer	0.01
HK_UPPER	Mol (lower) + Kasterlee sands	1
	Diest clayey zone	0.14
	Diest sands	1
	Dessel sands	0.1
HK_LOWER	Berchem + Voort sands	0.003

Table 3: Definition of combined hydraulic conductivity parameters for the upper and lower aquifer hydrogeologic units.

sands (the model goes down to the Boom Clay regional aquitard) that were adopted from the previous hydrogeological model. To avoid over-parameterization during model calibration, whereby strong correlation between units in the same aquifer (upper or lower) would eliminate the impact of non-sensitive parameters, the hydraulic conductivity parameters for the units pertaining to the upper, respectively lower aquifers were combined into two parameters: HK_UPPER and HK_LOWER. The hydraulic conductivity of the units that were used to determine one of the two combined parameters is calculated using a fixed ratio to the combined parameter value (Table 3). For example, the ratio of the Quaternary + Mol Upper hydraulic conductivity to HK_UPPER = 0.6. This approach is supported by the results of the exploratory data analyses.

The vertical anisotropy was fixed to 1 (isotropy assumed) for the upper aquifer hydrogeologic units. In case of the lower aquifer hydrogeologic units, an anisotropy of 3 was used for the Diest clayey layer and Diest sands (conform to the results of the site characterisation). Isotropic K-values were assumed for the Dessel and Berchem units. The latter assumption is inherited from the previous version of the model. In case of the Kasterlee Clay, the vertical anisotropy is one of the key modelling parameters, since vertical flow is assumed through this unit.

Three parameters were calibrated to achieve a good agreement between simulated and observed heads: HK_UPPER, HK_LOWER and the vertical anisotropy (VANI) of the Kasterlee Clay aquitard. The calibration was done for three different conceptual models of the Kasterlee Clay aquitard hydraulic conductivity spatial distribution:

1. K distribution based on CPT interpretation: Combination of two data sources was used to derive the spatial K distribution: the statistical analysis of K values from core samples and the interpretation of the CPT data. In the former analysis, three hydraulic conductivity peaks were identified (high, medium and low K), while in the latter interpretation, clayey, silty and sandy fractions were derived at each CPT location. The mean of the high, medium and low K classes were assumed to be representative, respectively for the sandy, silty and clayey fractions. In this way, we could calculate at each discrete CPT location the aquitard horizontal (using weighted mean) and vertical (using harmonic mean) K value using for each layer the layer thicknesses and the three size fractions (see Figure 11). The vertical anisotropy field was then calculated by dividing the horizontal K field by the vertical one. The vertical anisotropy parameter was set to 1000 and a multiplication field (vertical anisotropy field divided by 1000) was implemented into MODFLOW, whereby the final value of Kasterlee Clay vertical anisotropy in each cell was obtained by multiplying the Kasterlee Clay anisotropy parameter and corresponding value in the multiplication field. As mentioned earlier, the Kasterlee Clay vertical anisotropy parameter was subject of calibration.

2. Uniform K of the Kasterlee Clay aquitard: The Kasterlee Clay aquitard is characterized by a single horizontal hydraulic conductivity value and a single vertical anisotropy value. This approach is consistent with the previous version of the model. It represents an extremely simplified, yet more robust way of parameterization of the Kasterlee Clay unit, whereby a single value is calibrated and no attempts are made to determine the spatial variability of the parameter.
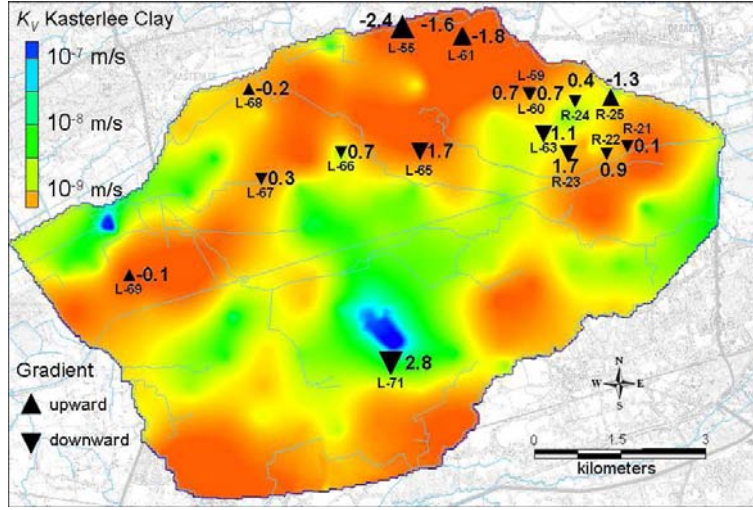
13

Figure 11: The Kasterlee Clay aquitard vertical hydraulic conductivity field based on CPT interpretation, and observed hydraulic gradients across the Kasterlee Clay aquitard.

3. Optimized K distribution based on thickness and hydraulic gradients: The Kasterlee Clay aquitard is divided into several zones based on the unit's thickness obtained from the CPT interpretations. The multiplication value for the vertical anisotropy (parameter VANI) within these zones was then manually calibrated to obtain the best possible fit of the observed heads (Figure 12). A single value of the Kasterlee Clay aquitard horizontal hydraulic conductivity was used.

The approach based on model 1 resulted in a large spatial variability in the aquitard K values (from $\approx 10^{-7}$ to $\approx 10^{-9}$ m/s; Figure 11). At some locations, notably in the vicinity of piezometer L-71, zones of high hydraulic conductivity were calculated. At the same location, a large average hydraulic gradient exists (2-8 m/m), which suggests a high resistance to flow owing to a low permeable aquitard. These apparent discrepancies resulted in a less good calibration compared to model 2 and 3. The CPT-based predictions of such high hydraulic conductivity zones needs further corroboration, but is likely due to an imprecise prediction of the clay and silt percentages using the model of Robertson & Campanella (1986) and the discrepancy between the hydraulic conductivity classes and these size fractions.

5 Results

For each K model for the aquitard, the calibration was performed using an automatic calibration (using UCODE; Poeter & Hill, 1999) starting from the values obtained from pumping tests (Table 4). Figure 13 shows the residuals (measured minus simulated values) for each calibration case. The resulting parameters for all calibration cases are given in Table 4 and the measured vs. simulated heads are shown in Figure 14.

Generally, good calibration is obtained in the upper aquifer (Figure 13, left), whereby the residuals are smaller than 0.5 meters in all calibration cases. Calibrating the lower aquifer contributes most to the error in the objective function. The goodness-of-fit statistic during calibration (sum of squared weighted residuals) improves considerably by changing the Kasterlee Clay aquitard hydraulic conductivity conceptualization. This points at the slightly better performance of model 3 compared to the first two conceptualizations of the Kasterlee Clay K field and the importance of this unit in the hydrogeology of the area.

The optimal parameters derived for the upper aquifer (Quaternary, Mol and Kasterlee units) are
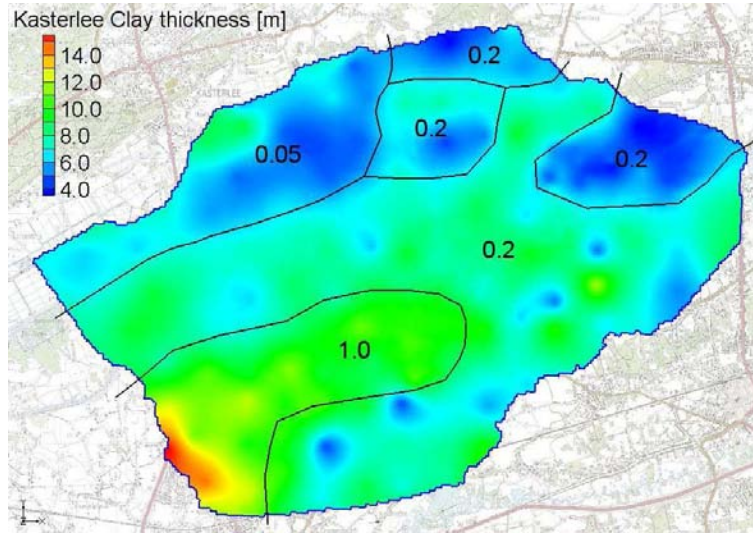
14

Figure 12: Manually delineated Kasterlee Clay aquitard vertical hydraulic conductivity zones, based on the unit thickness. The values within the zones are the Kasterlee Clay aquitard VANI multiplication parameter.

higher by approximately a factor 4 than the starting parameters based on the pumping test results (Table 4). In the lower aquifer, the difference is smaller, approximately by a factor 2. The combined hydraulic conductivity parameter of the lower aquifer is correlated with the parameter of the Kasterlee Clay aquitard vertical anisotropy. This correlation is the strongest in case of model 2 (i.e. the uniform K Kasterlee Clay conceptualization), explaining the difference in estimated value of the lower aquifer K value. The estimated parameters are generally higher than the values measured during the site characterisation. This may be due to the scale dependency of the K-parameter. The difference between directly measured and calibrated K is higher in case of the laboratory data than in case of the pumping test data and it is much larger in case of the strongly heterogeneous Kasterlee Clay aquitard than in case of the aquifers. For a better overview of calibration results, the parameter values are plotted in Figure 15. Indeed, the hydraulic conductivity seems to increase systematically from lab, to pump test, to calibrated parameter values. For the two deepest units however (Dessel and Berchem + Voort), the opposite seems to be true. The geometric mean of the lab-derived conductivities seems to be higher than their calibrated values. This might be due to the very limited number of samples of these units, which are all coming from one single borehole. The representativeness of these lab data can thus be questioned.

Despite the differences in the Kasterlee Clay aquitard conceptualization and its impact on the corresponding calibration, the updated model performs better than the previous version. With a larger number of observations, the highest absolute residual equals now 0.6 m (in case of conceptual model 3) against 1.5 m achieved previously. The average residual decreased from 0.25 m to 0.23 m, whereas the number of observations increased from 71 to 86. The model was steady-state, and a period of 20 years was used for the observations (1990-2010).
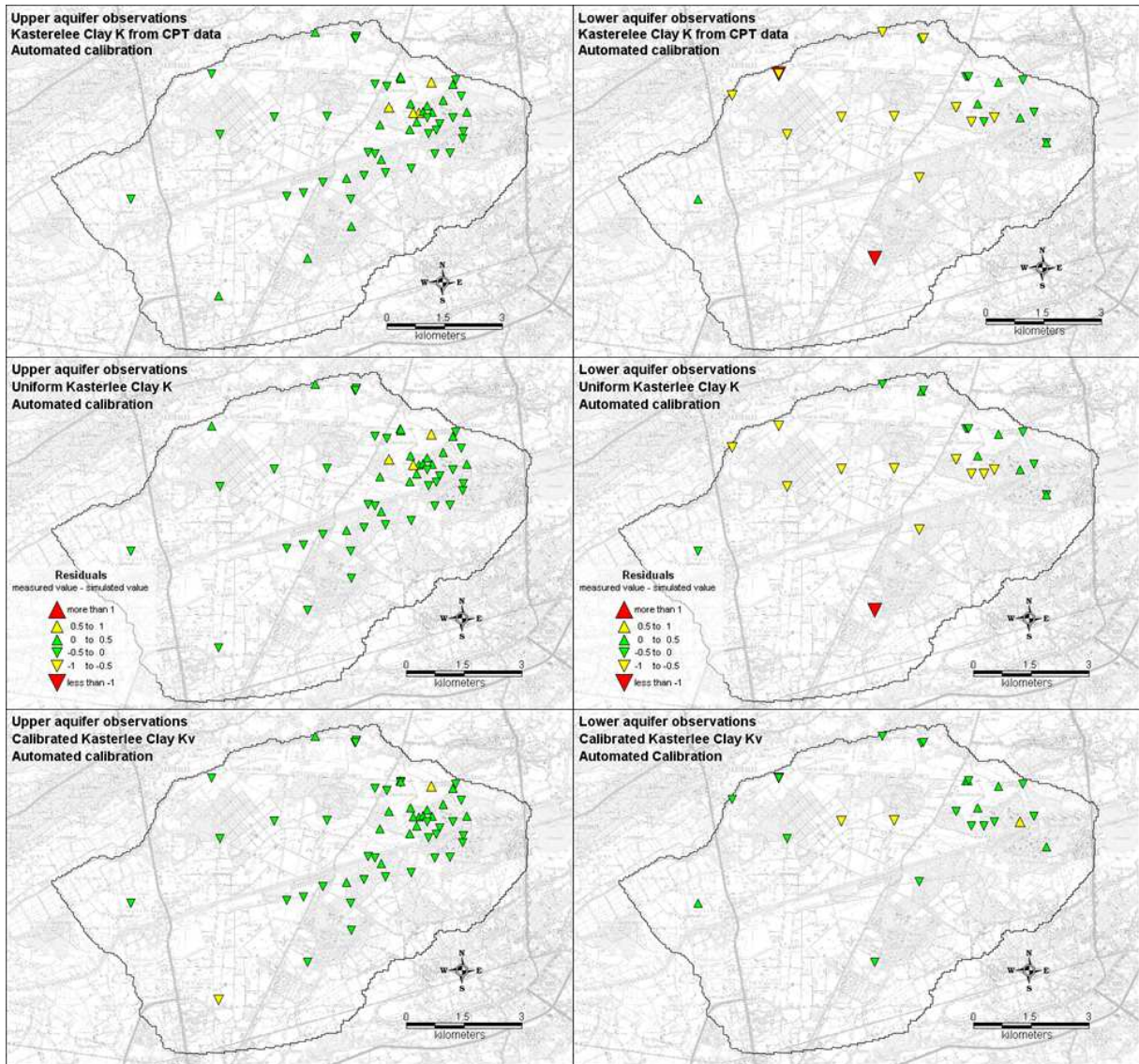
Figure 13: Residuals (measured − observed groundwater heads) for the upper aquifer (left) and lower aquifer (right) for 3 different conceptual models for the aquitard.
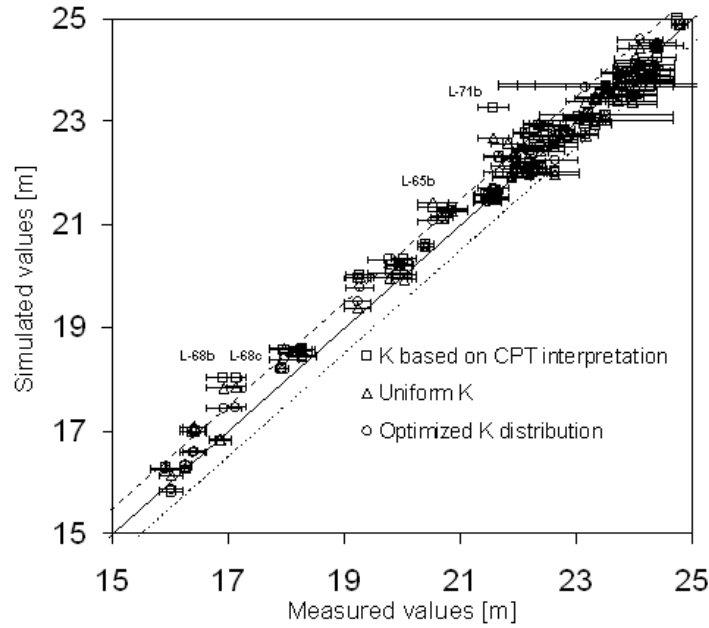
Figure 14: Measured versus simulated groundwater levels in the local flow model. Dashed lines represent ± 0.5 m from the full zero residual line. The error bars are calculated as the measurement ±σ (standard deviation).

Parameter	Lab geometric mean	Pump test (starting value)	Model 1	Model 2	Model 3
Quaternary + Mol (upper) [m/s]	9.28E-06	2.40E-05	7.70E-05	9.20E-05	8.20E-05
Mol clayey layer	/	2.70E-07	1.30E-06	1.50E-06	1.40E-06
Mol (lower) + Kasterlee	1.15E-05	4.10E-05	1.30E-04	1.50E-04	1.40E-04
Kasterlee Clay	6.72E-08	3.5E-8 - 5.4E-6[*]	3.5E-8 - 5.4E-6	2.90E-06	2.90E-06
Kasterlee Clay (VANI)	/	10 – 16200[*]	0.34 to 556.3	153.3	56 to 1112
Diest clayey zone	5.31E-06	6.50E-06	1.30E-05	8.10E-06	1.20E-05
Diest	1.69E-05	4.60E-05	9.20E-05	5.80E-05	8.40E-05
Dessel	2.27E-05	4.60E-06[*]	9.20E-06	5.80E-06	8.40E-06
Berchem + Voort	1.23E-06	1.20E-07[*]	2.80E-07	1.70E-07	2.50E-07
Recharge [mm/y]	/	295	295	295	295
Fit statistics					
Sum squared weighted residuals	/	/	62.5	51.5	24.8
R² (measured vs. simulated)	/	/	0.978	0.982	0.99

[*] Starting values **not** based on the pumping tests. The Kasterlee Clay K could not be estimated because of lack of hydraulic response across the aquitard. Starting values based on statistical analysis of lab tests. The K of units deeper than Diest were not tested and values from the previous model were reused.

Table 4: Parameter values and fit statistics for automatically calibrated model using three concepts of spatial distribution of the Kasterlee Clay hydraulic conductivity.
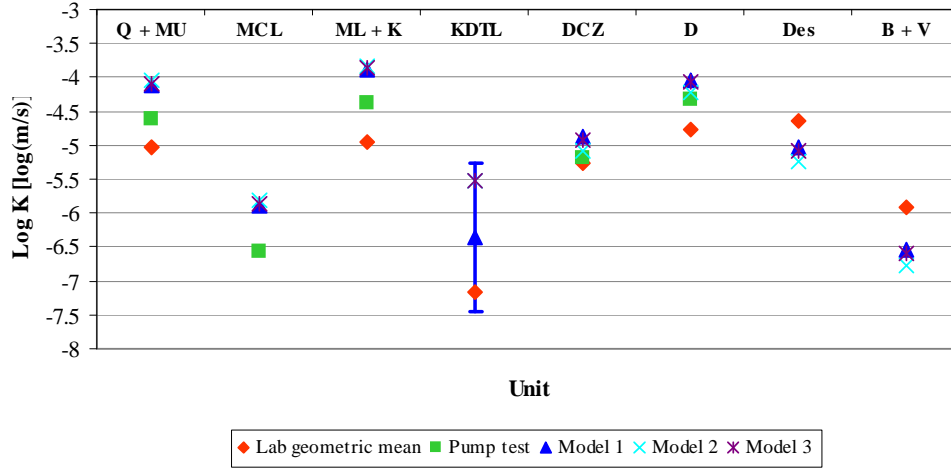
Figure 15: Parameter values for the different hydrostratigraphic units derived from different sources. (Q+MU: Quaternary + Mol Upper, MCL: Mol clay layer, ML+K: Mol Lower + Kasterlee, Kasterlee Clay: Kasterlee-Diest transition layer, DCZ: Diest clayey zone, D: Diest, Des: Dessel, B+V: Berchem + Voort)

6   Conclusion

The analysis of 8 50-m long cored boreholes in combination with nearly 180 CPT measurements allowed to create a detailed 3-dimensional hydrogeological model covering a study area of approximately 60 km². The incorporation of this information into a groundwater flow model followed by a calibration of the hydraulic conductivity for all hydrostratigraphic units resulted in a satisfactory modelling of the groundwater levels in an upper and lower aquifer. A critical component in the calibration was the clay-rich and heterogeneous aquitard. Three conceptual models were tested that each had a different way of dealing with the aquitard spatial variability in K. Although the most complex model, with spatially variable K-values based on interpretation of CPT data, has considerable prospect, it performed slightly worse than the spatially uniform model (uniform vertical and horizontal K-value) because the conversion of CPT data into K-values was done without proper calibration. The third model concept was based on a manual zonation of the thickness of the aquitard, and performed best.

Therefore, the next step for updating the groundwater flow model will be the full quantitative analysis, including calibration of the CPT parameters as a secondary variable in predicting the hydraulic conductivity of all the hydrogeological layers.

Acknowledgements

References

Anderman, E. R. & Hill, M. C. (2000). MODFLOW-2000, The US Geological Survey modular groundwater model—Documentation of the hydrogeologic-unit flow (HUF) package. mines.edu. Denver, Colorado.

Cressie, N. & Hawkins, D. M. (1980). Robust estimation of the variogram: I. Journal of the International Association for Mathematical Geology, 12(2), 115-125.

Gedeon, M. & Mallants, D. (2004). Hydrogeological model for the safety evaluation. Groundwater flow and transport calculations for the nuclear zone Mol-Dessel. Surface disposal of category A waste. Restricted Contract Report, SCK•CEN-R-3797, pp. 53, Mol

Gedeon, M. & Mallants, D. (2007). Hydrogeological modelling in support of site characterisation. Project near surface disposal of category A waste at Dessel. NIRAS-MP5-03 DATA-LT(HYD), Version 1, pp. 62

Gedeon, M. & Mallants, D. (2010). Prediction uncertainty in a multi-scale groundwater flow and transport model. IAHR 2010 Conference Paper.

Hamlett, J., Horton, R. & Cressie, N. (1986). Resistant and exploratory techniques for use in semivariogram analyzes. Soil Science Society Of America Journal, 50(4), 868-875.

Koltermann, C. & Gorelick, S. (1996). Heterogeneity in Sedimentary Deposits: A Review of Structure Imitating, Process Imitating, and Descriptive Approaches. Water Resour. Res, 32(9), 2617-2658.

Louwye, S., De Schepper, S., Laga, P. & Vandenberghe, N. (2007). The Upper Miocene of the southern North Sea Basin (northern Belgium): a palaeoenvironmental and stratigraphical reconstruction using dinoflagellate cysts. Geological Magazine, 144(1), 33-52

Mohanty, B., Kanwar, R. & Horton, R. (1991). A robust-resistant approach to interpret spatial behavior of saturated hydraulic conductivity of a glacial till soil under no-tillage system. Water Resources Research, 27(11), 2979-2992.

Mohanty, B.P. & Kanwar, R.S. (1994). Spatial variability of residual nitrate-nitrogen under two tillage systems in central Iowa: A composite three-dimensional resistant and exploratory approach. Water Resources, 30(2), 237-251.

Poeter, E.P. & Hill, M.C. (1999). UCODE, a computer code for universal inverse modelling. Computers & Geosciences, 25(4), 457-462

Robertson, P.K. & Campanella, R.G. (1986). Guidelines for use, interpretation and application of the CPT and CPTU. U B C Soil Mech, Series99, Civil Eng, Dep,, Vancouver

Wemaere, I., Beerten, K., Gedeon, M., Labat, S., Rogiers, B., Mallants, D., Salah, S., Leterme, B. (2010). Geological description and characterisation of the disposal site at Dessel Project near surface disposal of category A waste at Dessel. Project near surface disposal of category A waste at Dessel. NIROND-TR report 2009–05 E, pp. 279